ACS OMEGA

Article

Cite This: ACS Omega 2019, 4, 2973−2979

http://pubs.acs.org/journal/acsodf

Amine-Modified Mesoporous Magnesium Carbonate as an Effective Adsorbent for Azo Dyes

Maria Vall, Maria Strømme,* and Ocean Cheung*

Nanotechnology and Functional Materials Division, Department of Engineering Sciences, The Ångström Laboratory, Uppsala University, Box 534, SE-751 21 Uppsala, Sweden

Supporting Information

ABSTRACT: Mesoporous magnesium carbonate (MMC) was evaluated as a potential candidate material for removal of dyes from textile industry wastewater. The adsorption property of MMC was analyzed for three different azo dyes: reactive black 5 (RB5), amaranth (AM), and acid red 183 (AR183). Further, the effect of porosity, amine modification, ionic strength, and pH was evaluated. MMC modified with 3-(aminopropyl)-triethoxysilane (aMMC) showed consistently high uptake levels for all of the azo dyes tested; the uptake of RB5, AM, and AR183 was ∼360, ∼143 and ∼170 mg/g, respectively. The results demonstrated the importance of porosity and surface chemistry in the effective adsorption of the azo dye in aqueous systems. The uptake of RB5 and AM on aMMC was not significantly affected by pH (when varied between 4 and 10), although reduced uptake of RB5 and AM was observed at pH values <2 and >12. The addition of NaCl salt at concentrations up to 1000 mM had minimal effect on the high uptake of RB5 on aMMC. The uptake of AM by aMMC was reduced by approximately 20% in the presence of NaCl even at low concentrations. The uptake of AR183 by aMMC varied noticeably by changes in pH and no specific trend was observed. The presence of NaCl also adversely affected the uptake of AR183 on aMMC. The adsorption of the azo dye on aMMC was most likely driven by electrostatic interactions. We show here that aMMC is a potential candidate adsorbent for the effective removal of azo dyes from textile wastewaters.

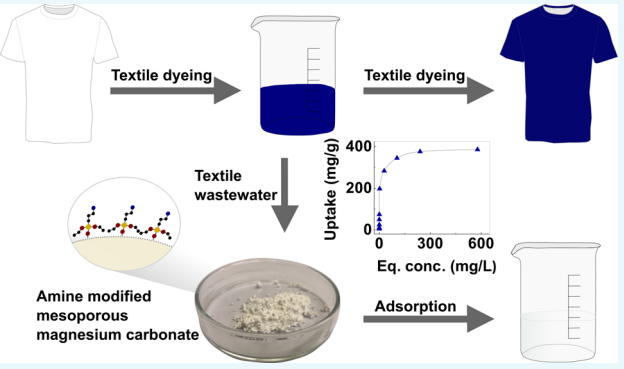

1. INTRODUCTION

The textile industry is one of the highest water-consuming industries in the world, using between 2.5 and 932 L of water per kg of fabric produced.[1] Water is needed in many of the steps in textile production, one particular process that requires a large amount of water is coloring.[1] During the coloring of textiles, different types of dyes and other additives are used in excess. This means that the wastewater from the process contains a large amount of dyes and additives. On average, 10−15% of the dyes used are still present in the effluent.[2]

Azo dyes are one of the most commonly used classes of textile dyes and constitute up to 70% of the total of dyes produced. They are organic compounds that have nitrogen−nitrogen double bonds (N═N). The popularity of azo dyes is related to their stability, the good variation of colors, and their low cost.[3] Some examples of typical azo dyes include Congo red, methyl orange, methyl red, reactive black 5, amaranth, and acid red 183. In this study, reactive black 5, amaranth, and acid red 183 (referred to as RB5, AM, and AR183, respectively, in the rest of this study) have been used. RB5 is one of the most common dyes for cotton and other cellulosic fibers;[4] AM is mainly used for dyeing textiles, but it has also been used as a coloring agent in the food and beverage industry.[5] AR183 is used as a wool and leather dye.[6]

Unfortunately, azo dyes also have some serious drawbacks. Reports of the toxicity of RB5 and AM have lowered their use in the textile industries and resulted in a total ban in some countries.[5] AR183 has also proven to be highly carcinogenic and very resilient toward degradation.[7] Furthermore, the discharge of azo dye containing wastewater into natural water sources can cause discoloration even at low concentrations. Azo dye containing wastewater will also interfere with light transmission through the water, which disturbs the aquatic ecosystem and is esthetically displeasing.[8] More importantly, many azo dyes are toxic to the environment and their metabolites (aromatic amines such as benzidine) are cancerogenic and can cause various types of human and animal tumors.[5,7,9] Studies have also shown that some azo dyes are cancerogenic even without being metabolized. Furthermore, some components of azo dyes, such as *p*-phenylenediamine, are allergens that can induce throat irritation, asthma, and dermatitis.[10] It is, therefore, of great interest to develop an effective and low-cost strategy to remove azo dyes from dye effluent waters.[8] The successful removal of azo dye from

Received: December 13, 2018
Accepted: January 29, 2019
Published: February 11, 2019

DOI: 10.1021/acsomega.8b03493
ACS Omega 2019, 4, 2973−2979

wastewater might also allow some of the wastewater to be reused if it meets other requirements of the process (linked to salt concentration, pH, metal ions, etc.) and, hence, lowers the overall consumption of water.

Several different methods have been proposed for the efficient removal of excess dye from the effluent. The methods can be divided into two groups: separation and degradation.[11] Examples of separation techniques are coagulation[12] and adsorption,[13,14] whereas biodegradation[15] and oxidation[11] are examples of degradation techniques. Adsorption is a promising method as it can easily be implemented in existing processes and will therefore be relatively cost-effective.[16] For the adsorption process to work efficiently, a good sorbent is required. A good adsorbent should have a high uptake of dye, be easy to produce in large quantities, and have a low cost. Porous materials are good candidate adsorbents as they have good adsorption qualities due to their high surface area. Various porous materials such as activated carbon,[17,18] mesoporous silica,[19,20] and zeolites[21] have been tested for adsorption of azo dyes previously.

Mesoporous magnesium carbonate (MMC) is a highly porous amorphous magnesium carbonate material first described in 2013[22] and has been produced in industrial scale since. MMC is made up of aggregated nanometer-sized particles (<10 nm) of amorphous $MgCO_3$ and MgO (with MgO content approximately 10−20 wt %). The porosity comes from the space between the aggregated particles. MMC has very high specific surface area (larger than 700 m^2/g), and the average pore size could be accurately controlled between 2 and 20 nm.[23] MMC is biocompatible and has proven to be noncytotoxic.[24] We have previously shown that the surface of MMC could be tailored by amine modification. Amine modification could be used to increase the stability of MMC by hindering crystallization as well as controlling the surface chemistry.[25] We also showed that the release rate of the anti-inflammatory drug ibuprofen could be controlled by varying the levels of amine coverage on the pore surface of MMC.[26]

In this study, we will evaluate MMC and amine-modified MMC (herein referred to as aMMC) as adsorbents for three azo dyes: RB5, AM, and AR183. Although MMC has been tested for various applications such as drug delivery and water adsorption, its application in adsorption of pollutants (e.g., azo dyes) from water has not yet been tested. The effect of amine modification of MMC, the pH, and the salt concentrations on the adsorption of azo dyes will be examined. Amine modification should enhance the adsorption of azo dyes as the amine groups on aMMC would be protonated at pH under their pK_a value, which would increase the affinity for the adsorption of anionic azo dyes.[27]

2. RESULTS AND DISCUSSION

The as-synthesized MMC, the amine-modified aMMC, and $aMgCO_3$ were characterized using powder X-ray diffraction (XRD), infrared spectroscopy, N_2 sorption, and scanning electron microscopy. The data are presented and discussed in the Supporting Information. Note that the characterization of MMC and aMMC has been discussed previously.[26]

2.1. Dye Adsorption. The adsorption isotherms of three azo dyes with equilibrium dye concentration up to 600 mg/L (RB5, AM, and AR183) on MMC and aMMC are displayed in Figure 2. $MgCO_3$, $aMgCO_3$, and MgO were also tested for their ability to adsorb the three azo dyes, and the adsorption isotherms are shown in Figure 2.

The uptake of RB5 was most predominant on aMMC (Figure 2). The maximum uptake of RB5 on aMMC was ∼360 mg/g under the test conditions (∼20 °C, 60 min exposure time). MgO also showed a noticeable uptake of RB5, with a high maximum uptake of ∼175 mg/g. $aMgCO_3$ showed some uptake of RB5, but the maximum uptake was much lower than that on aMMC and MgO. The other adsorbents ($MgCO_3$ and MMC) showed relatively low uptake of RB5 (less than 35 mg/g). A similar trend was observed for the adsorption on AM; aMMC took up more AM than the other tested adsorbents, with a high uptake of 142.4 mg/g (∼20 °C, 60 min). MgO also took up a relatively high amount of AM (∼80 mg/g, ∼20 °C, 60 min). The other adsorbents (MMC, $aMgCO_3$, and $MgCO_3$) showed relatively low uptake of AM (less than 60 mg/g), similar to that observed for RB5. Interestingly, the uptake of AR183 was the highest on MgO (∼200 mg/g, ∼20 °C, 60 min) and noticeably higher than that on aMMC (∼170 mg/g, ∼20 °C, 60 min). The other adsorbents showed low uptake of AR183 (less than 30 mg/g), similar to that observed for RB5 and AM. The dye uptake on aMMC can be compared to that on other adsorbents as shown in Table 1.

Table 1. Comparison of the Dye Uptake on aMMC with Other Adsorbents

Adsorbent	Uptake RB5 (mg/g)	Conditions	Reference
aMMC	360	20°C, 1h	This work
Bamboo carbon	447	Not specified	2
Bone char	157	Not specified	2
Active carbon F400	176	Not specified	2
Activated carbon	50	20°C, initial pH, 1h	28
Modified sepiolite	121	RT, 4h	29
Modified zeolite	61	RT, 4h	29
Adsorbent	**Uptake AM (mg/g)**	**Conditions**	**Reference**
aMMC	143	20°C, 1h	This work
$MgAlCO_3$ (LDH)	121	RT, pH 6.4, 24h	30
MgAlO (LDO)	967	RT, pH 6.4, 24h	30
Fe_3O_4@mZrO_2/Rgo	76.9	25°C, pH 2	31
Bottom ash	7.9	30°C, pH 2, 9h	32
Aqueous biphasic extraction chromatographic (ABEC) resins	30.4	1h	33
Adsorbent	**Uptake AR183 (mg/g)**	**Conditions**	**Reference**
aMMC	170	20°C, 1h	This work
MgO	200	20°C, 1h	This work
Boron industry waste	48.5	25°C, pH 3, 1h	34
Multiwalled carbon nanotubes	45	25°C, pH 6, 0.5h	35
Shells of bittim	33	35°C, 0.75h	36

Two conclusions were drawn from the dye adsorption isotherms shown in Figure 1. First, the importance of surface area was demonstrated by comparing the uptake of the tested azo dyes between aMMC and $aMgCO_3$, as well as between MMC and $MgCO_3$. The specific surface area of the different materials is shown in Table 2. In both cases, the material with high specific surface area showed increased dye uptake for all three dyes. At C_{eq} = ∼500 mg/L, the high surface area aMMC took up 385.8 mg/g of RB5, 142.4 mg/g of AM, and 168 mg/g of AR183. In contrast, the chemically similar but low-surface-area $aMgCO_3$ took up just 34.4 mg/g of RB5, 9.1 mg/g of AM, and 28 mg/g of AR183 at the same C_{eq}. A similar observation was made when considering the dye uptake of MMC and $MgCO_3$; at C_{eq} = ∼500 mg/L, the high surface area MMC took up 31.8 mg/g of RB5, 59.6 mg/g of AM, and 21.5 mg/g of AR183, all of which were noticeably higher than the uptake of these dyes on $MgCO_3$ (1.4 mg/g of RB5, 0.5 mg/g of AM, and 1.9 mg/g of AR183). Second, the surface chemistry of the adsorbent also played an important role; amine modification

DOI: 10.1021/acsomega.8b03493
ACS Omega 2019, 4, 2973−2979

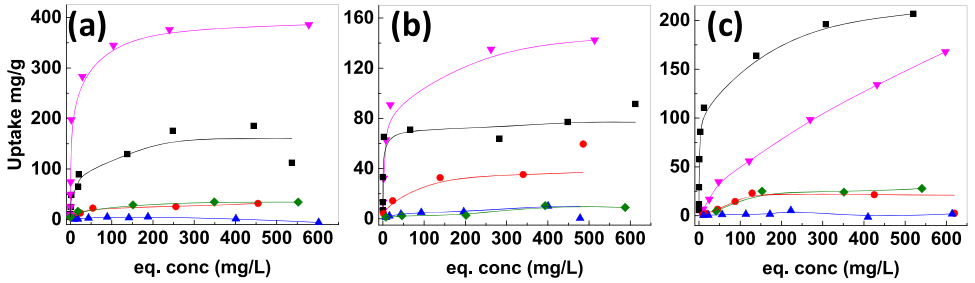

Figure 1. Adsorption isotherms for (a) RB5, (b) AM, and (c) AR183; (▼) aMMC, (■) MgO, (●) MMC, (▲) $MgCO_3$, and (♦) $aMgCO_3$. Note that the lines are drawn for clarity and do not represent the data points.

Table 2. BET Surface Area of the Samples Adsorption

sample	surface area BET (m^2/g)
MMC	660
aMMC	510
MgO (Sigma-Aldrich)	120
$MgCO_3$ (Sigma-Aldrich)	20
$aMgCO_3$	20

clearly enhanced the dye adsorption properties on MMC. This enhancement was demonstrated by comparing the dye uptake of aMMC and MMC. It is important to note that even with enhanced surface properties, high surface area is still required for good overall dye adsorption performance. This was demonstrated by $aMgCO_3$. $aMgCO_3$ had a higher uptake of AR183 and RB5 compared to that on $MgCO_3$, but the low surface area meant that the overall dye uptake was still lower than that of aMMC. Note that the high AR183 uptake on MgO also demonstrated the importance of surface interaction. The oxide surface was more favorable for the adsorption of AR183 than an amine surface, possibly due to the acidity of the Cr−OH group on AR183 that favored the adsorption on the basic oxide surface. In the rest of this study, we will focus our analysis on the adsorption of RB5, AM, and AR183 on aMMC only. Further analysis of the adsorption of AR183 on MgO (kinetics, effect of contact time, pH, and salts) can be found in the Supporting Information (Table S1 and Figures S1−S3).

The dye adsorption isotherms of aMMC were fitted with Langmuir, Freundlich, and Sips (Langmuir−Freundlich) models. The fitted parameters are presented in Table 3.

Table 3. Constants from Fits of the Adsorption Isotherms to the Three Different Models

		aMMC RB5	aMMC AM	aMMC AR183
Langmuir	R^2	0.9647	0.9917	0.9864
	q_e (mg/g)	357.298	141.512	284.392
Freundlich	R^2	0.9428	0.9158	0.9895
Sips	R^2	0.9942	0.9971	0.9906
	q_e (mg/g)	407.621	146.988	552.872
	n	0.477	0.743	0.747

When comparing the three different models, Sips gave the best fit for all cases with a high R^2 value for all of them. The Sips constant n was not 1 or close to 1 in any case, which indicated that the dye adsorption on aMMC could not be described as homogeneous. Electron micrographs, XRD diffractograms, and IR spectra of aMMC after adsorption are presented in the Supporting Information (Figures S4 and S5).

2.2. Kinetic Models. The adsorption kinetics of all three dyes on aMMC was investigated by monitoring the dye uptake every 10 min, up to 60 min. The kinetics of dye adsorption is presented in Figure 2, and the data points were normalized against dye uptake after 24 h (assumed to be 100%). The uptake of RB5 and AM on aMMC was relatively fast, with 50% of the uptake capacity reached between 10 and 20 min. Furthermore, more than 90% of the dye uptake capacity was reached within 60 min. In all cases except AR183 on aMMC, the uptake of dye increased with time. For AR183 on aMMC, there was an onset period of around 20 min during which the adsorption of AR183 on aMMC was close to 0. The low uptake of AR183 (when compared to that of MgO, Figures 2 and S3) on aMMC may be related to this onset period. The kinetics data were analyzed using the pseudo-first-[37] and pseudo-second-order[38] kinetic models (eqs 1 and 2)

Pseudo-first-order:

$$q_t = q_e(1 - e^{-kt}) \quad (1)$$

and

Pseudo-second-order:

$$q_t = \frac{q_e^2 kt}{1 + (q_e kt)} \quad (2)$$

with q_t being the amount adsorbed at time t (mg/g), q_{eq} being the amount adsorbed at equilibrium (mg/g) and k being the rate constant (1st order: min^{-1}, 2nd order: mg/g min).

Table 4 shows the fitted parameters using the two kinetic models. The pseudo-second-order kinetics model appeared to describe the adsorption of AM and RB5 on aMMC accurately. This was an indication that the rate-limiting step for adsorption in most cases was chemisorption and that the process was dependent on both the adsorbent and the adsorbate.[39,40] For adsorption of AR183 on aMMC, it appeared that neither kinetic models were able to describe the adsorption kinetics, which was expected due to the apparent onset time during the first 20 min. The parameters for the two models for the adsorption of AR183 on MgO are listed in the Supporting Information (Table S2).

2.3. Effect of pH. The effect of pH on the adsorption of the dye was investigated. Figure 3 shows the effect of initial pH of the dye solution on the uptake of RB5, AM, and AR183 on aMMC after 60 min exposure. In all three cases, the dye uptake diminished at pH 2. This was due to the fact that aMMC consisted predominantly of amorphous $MgCO_3$ with a small amount (~10−20 wt % relative to $MgCO_3$) of MgO (both are sensitive to low pH). The uptake of all three dyes on aMMC increased when the pH was increased. This was believed to be

DOI: 10.1021/acsomega.8b03493
ACS Omega 2019, 4, 2973−2979

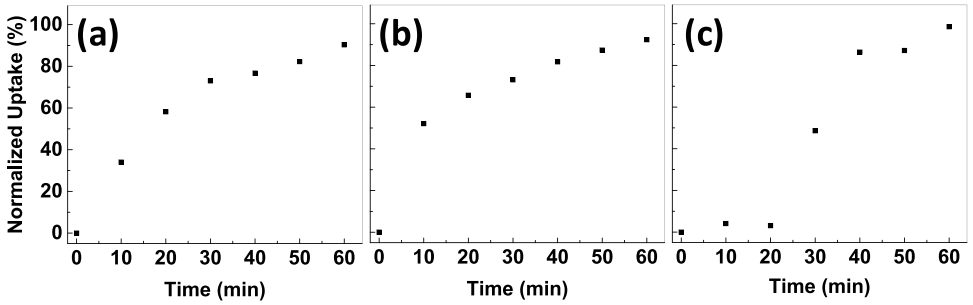

Figure 2. Kinetics of dye adsorption on aMMC: effect of contact time, normalized to the dye uptake after 24 h (100%). (a) RB5, (b) AM, and (c) AR183.

Table 4. Constants from Kinetic Models Calculated from the Kinetic Data of RB5, AM, and AR183 Adsorption on aMMC

		RB5	AM	AR183
R^2	pseudo-first	0.9950	0.9792	not possible
	pseudo-second	0.9941	0.9930	
q_e (mg/g)	pseudo-first	263.39	86.809	not possible
	pseudo-second	353.76	105.109	
k	pseudo-first	0.0473	0.0729	not possible
	pseudo-second	1.17×10^{-4}	7.96×10^{-4}	

due to protonation of the amine groups, which created a positively charged surface that could attract the negatively charged dye molecules. At pH > 10, the uptake decreased for RB5 and AM. This was probably related to the deprotonation of the amine groups that could occur at pH more than 10.[25] The uptake of AR183 on aMMC increased at high pH, the reason for this was not immediately clear to us. Further analyses are required to fully understand this observation.

2.4. Effect of Salt. Figure 4 shows that dye uptake on aMMC was affected by the presence of NaCl salt. The uptake of AM and AR183 noticeably decreased when the salt concentration was increased. The effect on RB5 adsorption on aMMC was less apparent. The relative uptake of RB5 on aMMC remained more than 90% of that in a salt-free environment. As the adsorption of dye on aMMC was driven by attractive electrostatic forces, the adsorbed amount would decrease with an increase in salt concentration due to a shielding effect. The effect was most profound on AR183. On the other hand, the uptake of RB5 was not significantly affected by the increased salt concentration.

3. CONCLUSIONS

MMC and the amine-modified aMMC have been tested as adsorbents for three commonly used azo dyes: RB5, AM, and AR183. aMMC showed high uptake of all three dyes with the equilibrium (C_{eq} ~ 500 mg/L) uptake reaching ~360 mg/g for RB5, ~143 mg/g for AM, and ~170 mg/g for AR183 with good uptake kinetics. More than 90% of the adsorption capacity (normalized to the dye uptake after 24 h) was reached within 60 min for all three dyes. Amine modification enhanced the uptake of dye on aMMC when compared to that on MMC, which demonstrated the importance of surface chemistry in the adsorption of azo dyes. The available surface area was also important for a high uptake of dye, as demonstrated by the significantly higher uptake of dyes on aMMC compared to that on amine-modified, low-surface-area $MgCO_3$. The uptake of RB5 and AM on aMMC was not noticeably affected by minor changes in pH (from 4 to 10). The presence of NaCl salt up to 1000 mM/L had minimal effect on the uptake of RB5 on aMMC, but a high salt concentration reduced the uptake of AM on aMMC by 20%.

High pH significantly increased the adsorption of AR183 on aMMC, whereas a high salt concentration had the opposite effect. Further studies are required to understand the specifics of the interaction between aMMC and AR183. We showed that aMMC is a candidate azo dye adsorbent with high uptake capacity and fast adsorption kinetics. The performance of

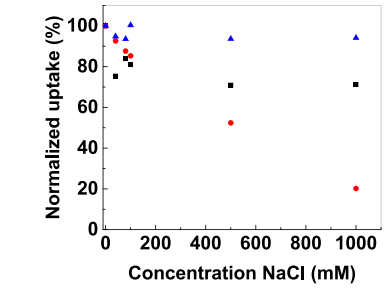

Figure 4. Effect of salt on adsorption of anionic dyes: RB5 (▲), AM (■), and AR183 (●).

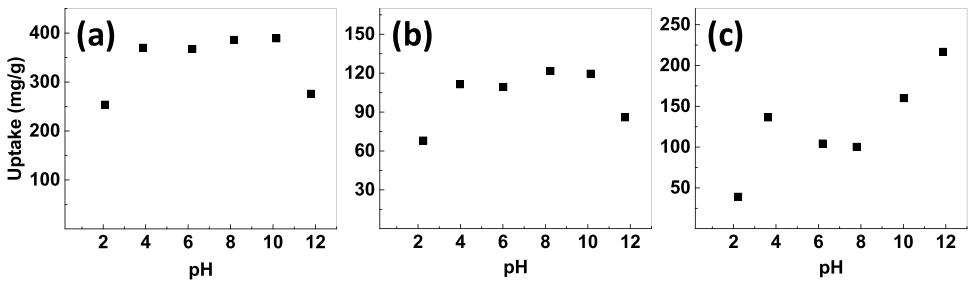

Figure 3. Effect of pH on the adsorption of (a) RB5, (b) AM, (c) AR183 on aMMC.

DOI: 10.1021/acsomega.8b03493
ACS Omega 2019, 4, 2973−2979

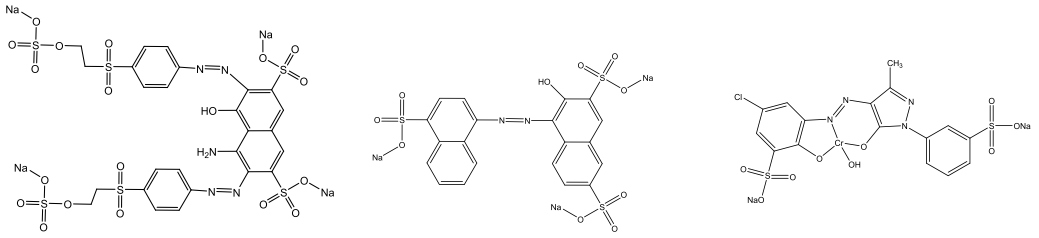

(a) (b) (c)

Figure 5. Structures of the three different dyes: (a) reactive black 5 (RB5), (b) amaranth (AM), and (c) acid red (AR183).

aMMC was not adversely affected by pH (for any of the three studied dyes) or the presence of salt (for two of the three dyes studied). The possibility for industrial-scale production of MMC and aMMC makes these materials interesting candidates for the treatment of textile wastewaters. A full-cost analysis as well as the development of a low-cost process for the production of aMMC will be essential for most applications of the material including that investigated in the present work.

4. MATERIALS AND METHODS

4.1. Materials. MgO (99% trace metal basis, 325 mesh), $MgCO_3$ (U.S.P.-grade), (3-aminopropyl)triethoxysilane (APTES, 98%), acid red 183 (30% dye content), amaranth (85−95% dye content), and reactive black 5 (≥50% dye content) were all purchased from Sigma-Aldrich; MeOH (HPLC-grade) was purchased from VWR Sweden.

4.2. Synthesis of Mesoporous Magnesium Carbonate (MMC). The procedure for synthesizing MMC was previously described in detail;[23] however, in short, 20 g of MgO was dispersed in 300 mL of MeOH and then pressurized with 4 bar of CO_2 for 24 h. The resulting gel was then centrifuged to remove unreacted MgO and then dried under constant stirring at 60 °C into a powder. The powder was further dried at 110 °C for additional 5 h.

4.3. Amine Modification of MMC. Amine grafting was carried out under dry conditions; all glassware was dried at 150 °C prior to the experiment, and the setup was continually flushed with dry N_2 gas for the duration of the experiment. The reaction was carried out under reflux; 5 g of MMC was dispersed in 300 mL of anhydrous toluene in a three-necked round bottled flask. The mixture was heated in an oil bath to 110 °C and was allowed to stabilize for 1 h; then, 8.5 mmol/g APTES was added. After 24 h, the solvent was removed by filtration and the material was washed with EtOH (2 × 50 mL). The modified MMC was then dried at 70 °C overnight to obtain dried aMMC. Surface modification on purchased $MgCO_3$ was carried out using the same procedures. Amine-modified $MgCO_3$ is referred to as $aMgCO_3$ in this study.

4.4. Dye Adsorption Studies. Dye adsorption studies were carried out at ambient room temperature, which was recorded to be ∼20 °C. Five different adsorbents (MMC, aMMC, $MgCO_3$, $aMgCO_3$, and MgO) and three different azo dyes (RB5, AM, and AR183) were tested. The chemical structure of the three different dyes is shown in Figure 5.

Standard dye solutions were made by dissolving 250 mg or 500 mg of dye in 250 mL of deionized water in a 250 mL volumetric flask; this gives standard solutions of 1000 or 2000 mg/L. Dye solutions used for the adsorption experiments were then made up by diluting the standard dye solutions with deionized water to the desired initial concentrations. Dye solutions (30 mL) of different concentrations were added to a 50 mL falcon tube, and 60 mg of adsorbent was added to the dye solution. The falcon tube was then placed on an orbital shaker (Heidolph Multi Reax, Schwabach, Germany) at 1000 rpm for 60 min at room temperature. After 60 min, the adsorbent and the dye solution were separated by centrifugation at 2500 rpm for 2 min. The final concentration of the dye solution after adsorption was then measured with UV−vis spectroscopy (Shimadzu UV1800) at the peak absorption wavelength of the dye (see Table 5) and compared to the initial concentration. The dye uptake of the adsorbents was then calculated according to eq 3.

Table 5. Peak Absorption Wavelengths for the Different Dyes

dye	wavelength (nm)
reactive black 5 (RB5)	598
amaranth (AM)	521
acid red 183 (AR183)	499

$$q = \frac{(C_0 - C_{eq})V}{m} \tag{3}$$

where C_0 (mg/L) is the initial concentration, C_{eq} (mg/L) is the measured concentration after 60 min, V (L) is the volume of the dye solution, and m (mg) is the mass of the adsorbent.

4.5. Fitting of Adsorption Isotherms. The dye adsorption isotherms of aMMC are fitted with the Langmuir, Freundlich, and Sips (Langmuir−Freundlich) models. The Langmuir equation[41] describes a monolayer adsorption to a homogenous surface with eq 4

$$q = \frac{q_e kC}{1 + (kC)} \tag{4}$$

Here, q is the uptake (mg/g), q_e is the equilibrium uptake (mg/g), k is the Langmuir isotherm constant (L/mg), and C is the equilibrium concentration (mg/L).

The Freundlich equation[42] better describes the properties of a heterogeneous system and is described by eq 5

$$q = kC_e^{1/n} \tag{5}$$

with q being the uptake (mg/g), C_e being the equilibrium concentration (mg/L), k being the Freundlich constant, and $1/n$ being the Freundlich exponent.

The Sips equation[43] is a combination of both Langmuir and Freundlich isotherms. It is described by eq 6

$$q = \frac{q_e kC^n}{1 + (kC^n)} \tag{6}$$

DOI: 10.1021/acsomega.8b03493
ACS Omega 2019, 4, 2973−2979

Here, q is the uptake (mg/g), q_e is the equilibrium uptake (mg/g), C is the equilibrium concentration (mg/L), k is the model constant (L/g), and the Sips constant n ($0 < n < 1$) represents the homogeneity of the system; a fully homogenous system will have an n value of 1, and eq 6 will become the Langmuir equation. A heterogeneous system will be represented with n lower than 1, with increased heterogeneity as n approaches 0.

4.6. Kinetics of Adsorption and Effect of Salt and pH.

Kinetic studies were carried out using the same procedures as listed above for selected adsorbents and dye concentrations. The dye concentration was monitored every 10 min for 60 min after adding the adsorbent to the dye solution. The effect of salt on dye adsorption was investigated for adsorbents with a high uptake of dye. NaCl was added to the dye solutions before the adsorption experiment, and the overall NaCl concentration was varied between 0 and 1000 mM. The effect of pH was evaluated for the adsorbents with a high uptake. The effect of pH was tested by adjusting the initial pH of the dye solutions with 0.1 M NaOH and 0.1 M HCl to values between 2 and 12 before the adsorption experiment. Dye adsorption experiment was then carried out using the same procedures as described above.

■ ASSOCIATED CONTENT

Supporting Information

The Supporting Information is available free of charge on the ACS Publications website at DOI: 10.1021/acsomega.8b03493.

Materials characterization; dye adsorption experiments; effect of contact time, pH, and salt concentration on the uptake of AR183 on MgO; SEM micrographs of aMMC; and XRD and IR spectra of aMMC (PDF)

■ AUTHOR INFORMATION

Corresponding Authors

*E-mail: Maria.Stromme@angstrom.uu.se (M.S.).
*E-mail: Ocean.Cheung@angstrom.uu.se (O.C.).

ORCID

Maria Strømme: 0000-0002-5496-9664
Ocean Cheung: 0000-0002-4072-4324

Notes

The authors declare no competing financial interest.

■ ACKNOWLEDGMENTS

The authors thank the Swedish Foundation for Strategic Environmental Research (Mistra) for its financial support (project name Mistra TerraClean, project number 2015/31). The Swedish Research Council (grant no. 2014-3929) and the Lars Hierta's Memorial Foundation are acknowledged for their financial support.

■ REFERENCES

(1) Dilaver, M.; Hocaoğlu, S. M.; Soydemir, G.; Dursun, M.; Keskinler, B.; Koyuncu, İ.; Ağtaş, M. Hot wastewater recovery by using ceramic membrane ultrafiltration and its reusability in textile industry. *J. Clean. Prod.* **2018**, *171*, 220−233.

(2) Ip, A. W. M.; Barford, J. P.; McKay, G. Reactive Black dye adsorption/desorption onto different adsorbents: Effect of salt, surface chemistry, pore size and surface area. *J. Colloid Interface Sci.* **2009**, *337*, 32−38.

(3) Saratale, R. G.; Saratale, G. D.; Chang, J. S.; Govindwar, S. P. Bacterial decolorization and degradation of azo dyes: A review. *J. Taiwan Inst. Chem. Eng.* **2011**, *42*, 138−157.

(4) El Bouraie, M.; El Din, W. S. Biodegradation of Reactive Black 5 by Aeromonas hydrophila strain isolated from dye-contaminated textile wastewater. *Sustainable Environ. Res.* **2016**, *26*, 209−216.

(5) Gupta, V. K.; Jain, R.; Mittal, A.; Saleh, T. A.; Nayak, A.; Agarwal, S.; Sikarwar, S. Photo-catalytic degradation of toxic dye amaranth on TiO_2/UV in aqueous suspensions. *Mater. Sci. Eng., C* **2012**, *32*, 12−17.

(6) Genc, A.; Oguz, A. Sorption of acid dyes from aqueous solution by using non-ground ash and slag. *Desalination* **2010**, *264*, 78−83.

(7) Saroj, S.; Kumar, K.; Pareek, N.; Prasad, R.; Singh, R. P. Biodegradation of azo dyes Acid Red 183, Direct Blue 15 and Direct Red 75 by the isolate Penicillium oxalicum SAR-3. *Chemosphere* **2014**, *107*, 240−248.

(8) Gupta, V. K. Suhas, Application of low-cost adsorbents for dye removal—A review. *J. Environ. Manage.* **2009**, *90*, 2313−2342.

(9) Singh, R. L.; Singh, P. K.; Singh, R. P. Enzymatic decolorization and degradation of azo dyes—A review. *Int. Biodeterior. Biodegrad.* **2015**, *104*, 21−31.

(10) Chung, K.-T. Azo dyes and human health: A review. *J. Environ. Sci. Health, Part C* **2016**, *34*, 233−261.

(11) Nidheesh, P. V.; Zhou, M.; Oturan, M. A. An overview on the removal of synthetic dyes from water by electrochemical advanced oxidation processes. *Chemosphere* **2018**, *197*, 210−227.

(12) Alinsafi, A.; Khemis, M.; Pons, M. N.; Leclerc, J. P.; Yaacoubi, A.; Benhammou, A.; Nejmeddine, A. Electro-coagulation of reactive textile dyes and textile wastewater. *Chem. Eng. Process.* **2005**, *44*, 461−470.

(13) Mohammadi, N.; Khani, H.; Gupta, V. K.; Amereh, E.; Agarwal, S. Adsorption process of methyl orange dye onto mesoporous carbon material−kinetic and thermodynamic studies. *J. Colloid Interface Sci.* **2011**, *362*, 457−462.

(14) Vahideh, P.; Hassan, H.; Khodabakhshi, A.; Morteza, S. Removal of dye from synthetic textile wastewater using agricultural wastes and determination of adsorption isotherm. *Desalin. Water Treat.* **2018**, *111*, 345−360.

(15) Barragán, B. E.; Costa, C.; Carmen Márquez, M. Biodegradation of azo dyes by bacteria inoculated on solid media. *Dyes Pigm.* **2007**, *75*, 73−81.

(16) Sharma, S. K. *Dyes Removal from Waste Water Using Green Technologies: Research Trends and Applications*; John Wiley & Sons, 2015.

(17) Al-Degs, Y. S.; El-Barghouthi, M. I.; El-Sheikh, A. H.; Walker, G. M. Effect of solution pH, ionic strength, and temperature on adsorption behavior of reactive dyes on activated carbon. *Dyes Pigm.* **2008**, *77*, 16−23.

(18) Tan, I. A. W.; Ahmad, A. L.; Hameed, B. H. Adsorption of basic dye on high-surface-area activated carbon prepared from coconut husk: Equilibrium, kinetic and thermodynamic studies. *J. Hazard. Mater.* **2008**, *154*, 337−346.

(19) Huang, C.-H.; Chang, K.-P.; Ou, H.-D.; Chiang, Y.-C.; Wang, C.-F. Adsorption of cationic dyes onto mesoporous silica. *Microporous Mesoporous Mater.* **2011**, *141*, 102−109.

(20) Chen, J.; Sheng, Y.; Song, Y.; Chang, M.; Zhang, X.; Cui, L.; Meng, D.; Zhu, H.; Shi, Z.; Zou, H. Multimorphology mesoporous silica nanoparticles for dye adsorption and multicolor luminescence applications. *ACS Sustainable Chem. Eng.* **2018**, *6*, 3533−3545.

(21) Alver, E.; Metin, A. Ü. Anionic dye removal from aqueous solutions using modified zeolite: Adsorption kinetics and isotherm studies. *Chem. Eng. J.* **2012**, *200−202*, 59−67.

(22) Forsgren, J.; Frykstrand, S.; Grandfield, K.; Mihranyan, A.; Strømme, M. A template-free, ultra-adsorbing, high surface area carbonate nanostructure. *PLoS One* **2013**, *8*, No. e68486.

(23) Cheung, O.; Zhang, P.; Frykstrand, S.; Zheng, H.; Yang, T.; Sommariva, M.; Zou, X.; Strømme, M. Nanostructure and pore size control of template-free synthesised mesoporous magnesium carbonate. *RSC Adv.* **2016**, *6*, 74241−74249.

DOI: 10.1021/acsomega.8b03493
ACS Omega 2019, 4, 2973−2979

(24) Frykstrand, S.; Forsgren, J.; Zhang, P.; Strømme, M.; Ferraz, N. Cytotoxicity, in vivo skin irritation and acute systemic toxicity of the mesoporous magnesium carbonate Upsalite. *J. Biomater. Nanobiotechnol.* **2015**, *6*, No. 257.
(25) Pochard, I.; Vall, M.; Eriksson, J.; Farineau, C.; Cheung, O.; Frykstrand, S.; Welch, K.; Strømme, M. Amine-functionalised mesoporous magnesium carbonate: Dielectric spectroscopy studies of interactions with water and stability. *Mater. Chem. Phys.* **2018**, *216*, 332−338.
(26) Vall, M.; Zhang, P.; Gao, A.; Frykstrand, S.; Cheung, O.; Strømme, M. Effects of amine modification of mesoporous magnesium carbonate on controlled drug release. *Int. J. Pharm.* **2017**, *524*, 141−147.
(27) Qin, Q.; Ma, J.; Liu, K. Adsorption of anionic dyes on ammonium-functionalized MCM-41. *J. Hazard. Mater.* **2009**, *162*, 133−139.
(28) Eren, Z.; Acar, F. N. Adsorption of Reactive Black 5 from an aqueous solution: equilibrium and kinetic studies. *Desalination* **2006**, *194*, 1−10.
(29) Ozdemir, O.; Armagan, B.; Turan, M.; Çelik, M. S. Comparison of the adsorption characteristics of azo-reactive dyes on mezoporous minerals. *Dyes Pigm.* **2004**, *62*, 49−60.
(30) Abdellaoui, K.; Pavlovic, I.; Bouhent, M.; Benhamou, A.; Barriga, C. A comparative study of the amaranth azo dye adsorption/desorption from aqueous solutions by layered double hydroxides. *Appl. Clay Sci.* **2017**, *143*, 142−150.
(31) Jiang, H.; Chen, P.; Zhang, W.; Luo, S.; Luo, X.; Au, C.; Li, M. Deposition of nano Fe_3O_4@mZrO_2 onto exfoliated graphite oxide sheets and its application for removal of amaranth. *Appl. Surf. Sci.* **2014**, *317*, 1080−1089.
(32) Mittal, A.; Kurup, L.; Gupta, V. K. Use of waste materials—Bottom Ash and De-Oiled Soya, as potential adsorbents for the removal of Amaranth from aqueous solutions. *J. Hazard. Mater.* **2005**, *117*, 171−178.
(33) Huddleston, J. G.; Willauer, H. D.; Boaz, K. R.; Rogers, R. D. Separation and recovery of food coloring dyes using aqueous biphasic extraction chromatographic resins. *J. Chromatogr. B: Biomed. Sci. Appl.* **1998**, *711*, 237−244.
(34) Atar, N.; Olgun, A.; Wang, S.; Liu, S. Adsorption of anionic dyes on boron industry waste in single and binary solutions using batch and fixed-bed systems. *J. Chem. Eng. Data* **2011**, *56*, 508−516.
(35) Wang, S.; Ng, C. W.; Wang, W.; Li, Q.; Li, L. A comparative study on the adsorption of acid and reactive dyes on multiwall carbon nanotubes in single and binary dye systems. *J. Chem. Eng. Data* **2012**, *57*, 1563−1569.
(36) Aydın, H.; Baysal, G. Adsorption of acid dyes in aqueous solutions by shells of bittim (Pistacia khinjuk Stocks). *Desalination* **2006**, *196*, 248−259.
(37) Lagergren, S. About the theory of so-called adsorption of soluble substances. *K. Sven. Vetensk.-Akad. Handl.* **1898**, *24*, 1−39.
(38) Ho, Y. S.; McKay, G. Pseudo-second order model for sorption processes. *Process Biochem.* **1999**, *34*, 451−465.
(39) Abramian, L.; El-Rassy, H. Adsorption kinetics and thermodynamics of azo-dye Orange II onto highly porous titania aerogel. *Chem. Eng. J.* **2009**, *150*, 403−410.
(40) Iram, M.; Guo, C.; Guan, Y.; Ishfaq, A.; Liu, H. Adsorption and magnetic removal of neutral red dye from aqueous solution using Fe_3O_4 hollow nanospheres. *J. Hazard. Mater.* **2010**, *181*, 1039−1050.
(41) Langmuir, I. The adsorption of gases on plane surfaces of glass, mica and platinum. *J. Am. Chem. Soc.* **1918**, *40*, 1361−1403.
(42) Freundlich, H. *Kapillarchemie: eine Darstellung der Chemie der Kolloide und verwandter Gebiete*; Akademische Verlagsgesellschaft, 1922.
(43) Sips, R. On the structure of a catalyst surface. II. *J. Chem. Phys.* **1950**, *18*, 1024−1026.

DOI: 10.1021/acsomega.8b03493
ACS Omega 2019, 4, 2973−2979